ELSEVIER

Dolomitic limes: evolution of the slaking process under different conditions

J. Lanas, J.I. Alvarez*

Departamento de Química, Facultad de Ciencias, Universidad de Navarra, C/Irunlarrea s/n, 31080 Pamplona, Spain

Abstract

Dolomitic lime-based pastes were prepared in order to study the evolution of the compounds during the slaking process. Thermal studies as well as X-ray diffraction and FT-IR spectroscopy were used to confirm the formed compounds.

The rate of the hydration of calcium and magnesium oxides has been determined under different conditions: atmospheric conditions, CO_2-rich and enclosed environment without CO_2. Also the lime powder evolution without water added was studied. Whereas CaO hydrates at a higher rate, MgO is very dependent by its particle size distribution and stirring.

The paper also focuses on the carbonation process. Given that carbonation is the most usual hardening process in lime pastes, its knowledge is necessary to understand the mechanical behavior of these pastes.

In an excess of water, calcium hydroxide carbonates giving calcite if exposed to CO_2. In lime powder, another mechanism has been established through vaterite formation. Magnesium hydroxide does not carbonate under normal conditions. In a CO_2 atmosphere nesquehonite ($MgCO_3 \cdot 3H_2O$) has been checked found as a result of carbonation.

1. Introduction

Dolomitic lime has been used for mortar preparation. In historical-artistic construction mortars containing dolomitic lime are less abundant than the aerial lime mortars. Nevertheless, the complexity of the system $CaO–MgO–H_2O–CO_2$ [1] and the variety of compounds involved in dolomitic limes pastes justify their scientific interest. Some previous works have discussed the composition of ancient dolomitic lime-based mortars [2–4]. Different phases such as calcite, magnesite, dolomite, hydromagnesite, brucite, portlandite, periclase and nesquehonite have been pointed out as constituents of the mortars. In previous work by our research group, the controversy about the occurrence of hydromagnesite ($Mg_5(CO_3)_4(OH)_2 \cdot 4H_2O$) (HY) has been highlighted [5]. In the aforementioned paper, it was stated that further studies will be necessary with the aim to clarify the conditions of the occurrence of HY in pastes of dolomitic origin.

This requirement can be applicable to the other compounds, because it is not clear which of them could be formed during the slaking, setting and hardening of dolomitic lime-based pastes. Botha and Strydom [6] reported synthetic preparations of magnesium hydroxy carbonate, and stated the difficulties in choosing experimental conditions. The complexity in knowing the compounds formed prior to developing the experiment lies in the great number of magnesium carbonates with very close chemical composition that can be obtained due to $MgO–CO_2–H_2O$ system (or $MgO–CaO–CO_2–H_2O$ system in the present paper). Nesquehonite ($MgCO_3 \cdot 3H_2O$), hydromagnesite ($Mg_5(CO_3)_4(OH)_2 \cdot 4H_2O$), dypingite ($Mg_5(CO_3)_4(OH)_2 \cdot 5H_2O$), lansfordite ($MgCO_3 \cdot 5H_2O$), artinite ($Mg_2CO_3(OH)_2 \cdot 3H_2O$), huntite ($Mg_3Ca(CO_3)_4$), magnesite ($MgCO_3$) and dolomite ($CaMg(CO_3)_2$) have been described. [1]. The interconversion between some of these compounds strictly depends of the conditions of reaction (temperature, CO_2 concentration, pH, RH) [6,7]. Furthermore, several unidentified magnesium carbonates have been reported, sometimes with amorphous structures [6–9].

* Corresponding author. Tel.: +34-948-425600; fax: +34-948-425649.
E-mail address: jalvarez@unav.es (J.I. Alvarez).

This paper also focuses on other important aspects, such as the rate of $Mg(OH)_2$ formation during the slaking of the burned lime, the influence of a CO_2 atmosphere, and the effect of the amount of water during the paste preparation. The knowledge about these factors is critical to understand the behavior of repair dolomitic lime-based mortars made with these pastes, specially the mechanical behavior.

In the present work, a commercial light calcined dolomite (LCD) has been slaked and studied at 20 °C. In order to analyze a totally calcined dolomite, the LCD was also burned, then slaked and kept under different conditions (atmospheric environment, CO_2-rich and enclosed environment without CO_2). The evolution of lime powder in an atmospheric environment was also studied. In order to characterize the chemical compounds formed in pastes made with these kind of limes, XRD and thermal studies were performed at different processing days. The influence of the different processing conditions and the rate of formation of components have also been discussed, specially the hydration of calcium and magnesium oxides and the carbonation process.

These results will be necessary in a further study about the mechanical behavior of repair dolomitic lime-based mortars.

2. Experimental work

2.1. Lime preparation

A commercial dolomitic lime of the class DL 85 according to European normative [10] was used, and it has been supplied by Dolomitas del Norte (Santullán, Cantabria). Table 1 gives its chemical characterization (according to European Standard) [11] and Fig. 1 (at day 0) shows its X-ray diffractogram.

Table 1
Chemical analysis of the main components of the LCD[a,b]

Lime	LCD
IL[c] (%)	5.00
SiO_2 (%)	0.00
CaO (%)	58.00
MgO (%)	36.00
R_2O_3[d] (%)	0.40
SO_3 (%)	0.26
Na_2O (%)	0.08
K_2O (%)	0.04

[a] Percentages related to dry lime.
[b] The methods specified by the European Standard EN-196 were followed for the chemical analyses.
[c] Ignition loss, indicates the weight loss due to calcination at 975–1000 °C.
[d] R_2O_3 expresses the percentage of Fe, Al and Ti as oxides.

As the results show, this is a light calcined dolomite on account of the content of dolomite and calcite. In order to achieve a dolomitic quicklime, this LCD was burned at 850 °C for 72 h. After this calcination the lime was sieved through a 0.5 mm sieve, and then burned again for 12 h more at 850 °C. The result of this calcination was a dolomitic quicklime (DQ) made up of CaO and MgO as the main components (Fig. 2, at day 0). Fig. 3 shows the limes obtained and processed with their characteristics.

2.2. Lime processing

2.2.1. Slaking process of the LCD

A metallic tray of 45 cm × 30 cm × 8 cm was used for slaking 2 kg of the light calcined dolomite. This slaking was conducted in an atmospheric environment at 20 °C and with discontinuous stirring. The initial addition of 3.5 L of water, at ∼20 °C, was added to obtain a lime putty (Fig. 3).
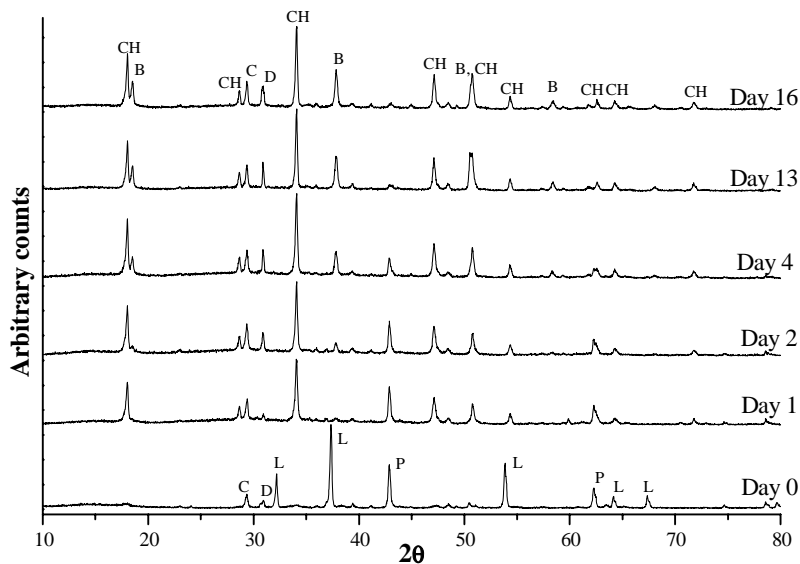

Fig. 1. XRD of LCD slaking evolution (atmospheric environment) at different days—B: brucite (ICDD 44-1482); C: calcite (ICDD 05-0586); CH: portlandite (ICDD 44-1481); D: dolomite (36-0426); P: periclase (ICDD 45-0946); L: calcium oxide (ICDD 37-1497).
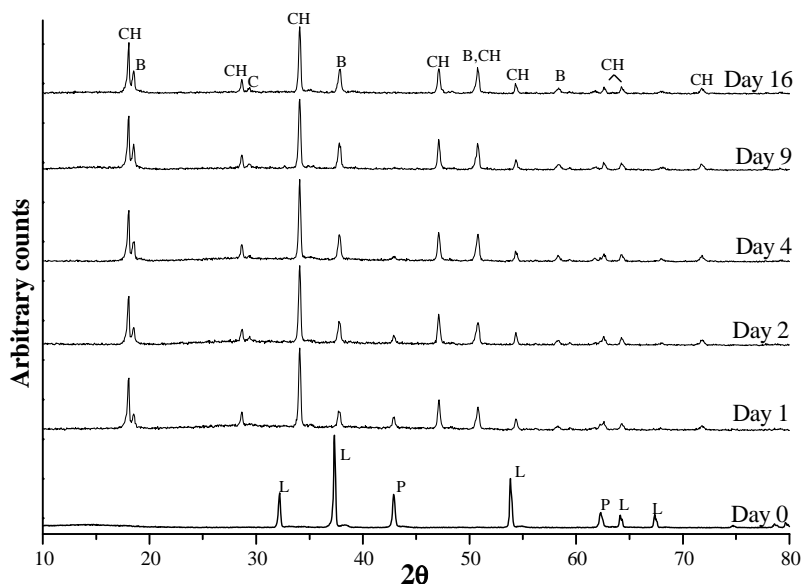
Fig. 2. XRD of DQ slaking evolution (atmospheric environment) at different days—B: brucite (ICDD 44-1482); C: calcite (ICDD 05-0586); CH: portlandite (ICDD 44-1481); P: periclase (ICDD 45-0946); L: calcium oxide (ICDD 37-1497).

2.2.2. Slaking process of the DQ

2.2.2.1. Atmospheric environment.
A glass reactor with a capacity of 2 L has been used to slake the DQ. Three hundred grams of this dolomitic quicklime was hydrated with the initial addition of 600 mL of water at $\sim$20 °C until a slaked dolomitic lime putty was produced. During the slaking process the lime putty was stirred three times a day for 1 min.

2.2.2.2. Enclosed environment without CO_2.
A mass of 300 g of DQ were hydrated in a closed glass reactor of 2 L (in order to avoid the contact between the lime and the atmospheric CO_2), with the initial addition of 725 mL of water at $\sim$20 °C until a putty was obtained. The bulk of the lime putty was continuously stirred with a Heidolph Stirrer RZR 2021 at a speed of $\sim$350 rpm.
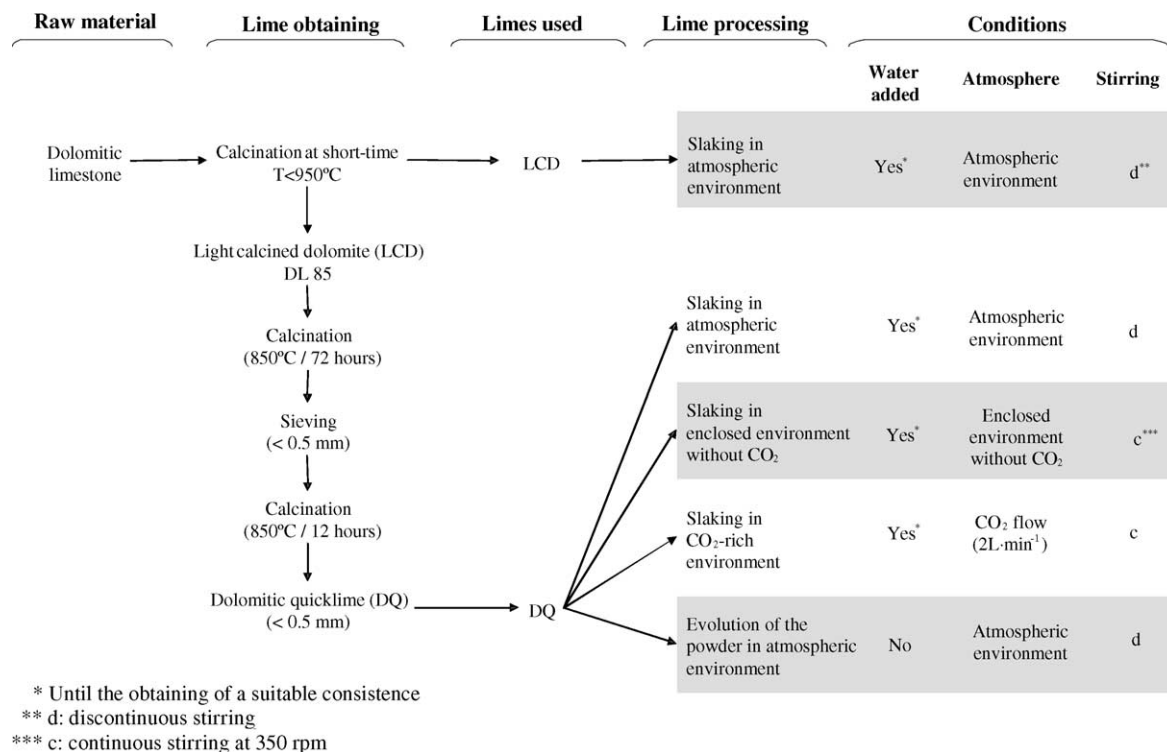

Fig. 3. Scheme of the different limes treatment.

2.2.2.3. CO₂-rich environment. An initial volume of 750 mL of water at ~20 °C was added to 300 g of DQ to obtain a lime putty. This process was conducted in a glass reactor of 2 L, with continuous stirring (Heidolph Stierrer RZR 2021 at ~350 rpm of speed) and a continuous CO_2 flow (2 L min⁻¹) (Fig. 3).

2.2.3. Evolution in atmospheric environment of the DQ powder

The DQ powder was exposed in a metallic tray of 16 cm × 11 cm × 4 cm to the atmospheric environment with discontinuous stirring.

2.3. Analytical methodology

2.3.1. Mineralogical analysis

During the different processes, lime putties and DQ powder were studied in order to determine the mineralogical components contained in the samples and the occurrence of new phases at different times. These analyses were carried out by means of X-ray diffraction (XRD) using a Bruker D8 Advance diffractometer (Karlsruhe, Germany), according to the diffraction powder method, with a Cu Kα_1 radiation and 0.05° 2θ increments at a rate of 0.1 s per step, scanned from 10° to 80° 2θ. The results were compared with the ICDD database.

2.3.2. Thermal analysis

Differential thermal and thermogravimetric analysis (DTA–TG) were conducted at different processing times using a simultaneous TGA-sDTA 851 Mettler Toledo thermoanalyzer (Schwerzenbach, Switzerland) with alumina crucibles, fitted with holed lids, at a 20 °C min⁻¹ heating rate, under static air atmosphere, from ambient temperature to 1200 °C. These techniques were used to quantify some compounds such us $Mg(OH)_2$ and $Ca(OH)_2$, through their dehydrations at ~400 and ~480 °C [12], or $CaCO_3$ and $CaMg(CO_3)_2$, through their decarbonations between ~600 and 900 °C [13]. Also thermal studies help to identify other compounds such us nesquehonite, hydromagnesite or magnesite, as later discussed.

2.3.3. Infrared spectroscopy

Powdered samples were analyzed by FT-IR spectroscopy, using KBr pellets. The analysis was performed with a Nicolet-FTIR Avatar 360, with OMNIC E.S.P. software. The resolution was 2 cm⁻¹ and the spectra were the result of averaging 100 scans. All measurements were carried out at 20 ± 1 °C and ca. 40% RH.

2.3.4. Particle size distribution

The particle diameters of the DQ and LCD and their distribution were determinate by a Malvern Particle Analyzer Mastersizer S using isopropanol as carried liquid.

3. Results and discussion

3.1. Evolution of the LCD slaking

As mentioned, the LCD contains calcium and magnesium oxides (CaO and MgO) as the main compounds (Fig. 1, at day 0). Also, traces of calcite (C), dolomite (D) and portlandite (CH) were observed. A slight calcination process due to the low temperature achieved and to the short residence time in the kiln explains the occurrences of C and D, because inside of the raw calcareous rock adequate temperature could not be reached for complete carbonation. However, the small amount of CH probably is formed due to a reaction with atmospheric moisture.

The slaking process has been carried out with the aim to study the rate of MgO and CaO hydrations and the new compounds formed. As the XRD results show (Fig. 1), 24 h after the 1st water addition, all the CaO was converted into CH. This is in agreement with previous work, it clearly indicates the high rate of CaO hydration [14].

However, the MgO hydration appears to be a slower process. In the literature it has been stated that a high temperature of dolomite decomposition inhibits the $Mg(OH)_2$ formation [15]. Also the specific surface area (related to the time and temperature of calcination), the particle size and the stirring speed have been highlighted as factors affecting the MgO reactivity [16].

In the present work, the LCD used possessed a relatively small particle size (Fig. 4 shows the particle size distribution of the LCD powder, having a trimodal distribution with maxima values at 60 μm (highest percentage), 2 and 0.25 μm) and it has been produced from a calcination temperature below 950 °C. Therefore, if no sintering occurred during calcination MgO would be chemically active.

XRD results show a slow hydration process: 2 days after water addition are required to confirm the $Mg(OH)_2$
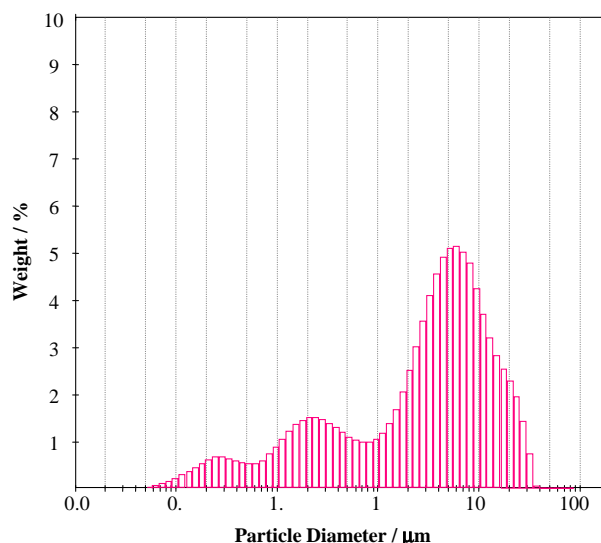
Fig. 4. Particle size distribution of the LCD powder.

formation (Fig. 1). The slaking was confirmed until almost all MgO disappeared (in traces by XRD) (16 days).

A slight formation of C and D can also be observed by XRD. In the beginning, LCD presented traces of C and D. Owing to the characteristics of the slaking, the atmospheric CO_2 in contact with the paste could cause a certain degree of carbonation, giving C and D. This carbonation could be facilitate by C and D this initial presence, through a syntaxial growth process that provides nucleating sites [17,18].

TG–DTA results confirm the XRD analysis. Fig. 5 shows the CH stabilization since the first day, and the continuous $Mg(OH)_2$ formation. Apart from the percentage variation between 0 and 24 h of the CO_2 (due to the water addition), a subsequent increase in carbonated materials has been also determined due to the increase of the percentage of CO_2. These TG results have been obtained taking into account the $Mg(OH)_2$ dehydration ($\sim$400 °C), the $Ca(OH)_2$ dehydration ($\sim$480 °C), and the decarbonations of C and D ($\sim$600–900 °C) [12,13].

3.2. Evolution of the DQ slaking

As mentioned before, XRD only detect calcium and magnesium oxides in the DQ after burning (Fig. 2, at day 0).

3.2.1. Atmospheric environment

Fig. 2 shows the XRD results at different test days. During DQ slaking, 24 h after the first water addition, CH appears. $Mg(OH)_2$ can be detected since day 1 in appreciable amounts, and at day 9 no MgO was formed. Therefore, the rate of MgO hydration turns out to be faster in DQ than in LCD, and total MgO slaking is observed.

These differences in the rate of reaction and MgO reactivity can be explained taking into account: the smaller DQ
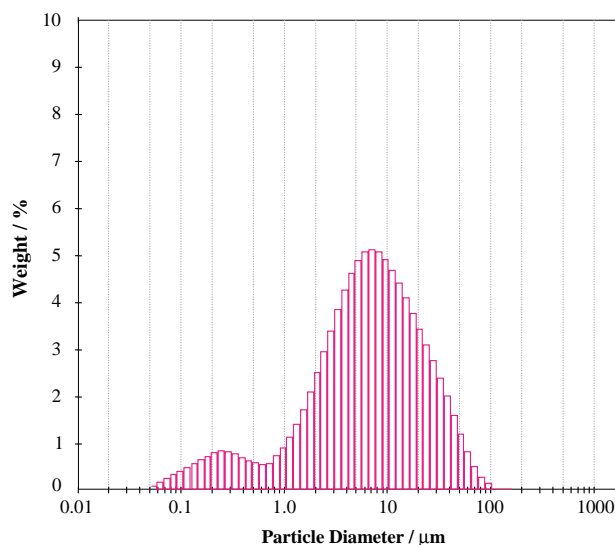

Fig. 6. Particle size distribution of the DQ powder.

particle size (higher specific surface) that increases its reactivity and accelerates the hydration. Fig. 6 presents the particle size distributions of DQ powder and the lower particle diameter is clearly distinguishable (bimodal distribution with maxima values at 7 μm as the highest percentage) as compared to LCD (60 μm as the highest percentage) (Fig. 4). The specific surface has been calculated and also differs: 0.78 $m^2 g^{-1}$ for LCD and 1.22 $m^2 g^{-1}$ for DQ.

A certain degree of carbonation is proved by the C diffraction peaks. Through thermogravimetric results, an increase in $CaCO_3$ is observed (Fig. 7). Dolomite phases have not been observed by XRD or TG–DTA analyses in DQ.

These facts are in contradiction with the smaller particle size of oxides in DQ, because they would give hydroxides with smaller particle size, which are more reactive.
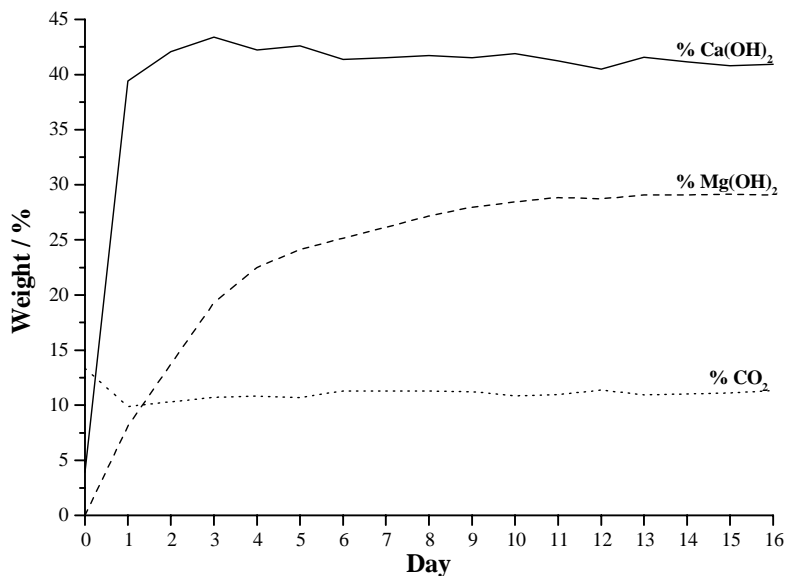

Fig. 5. Weight percentage of the compounds from TG results for LCD slaking (atmospheric environment) vs. time.
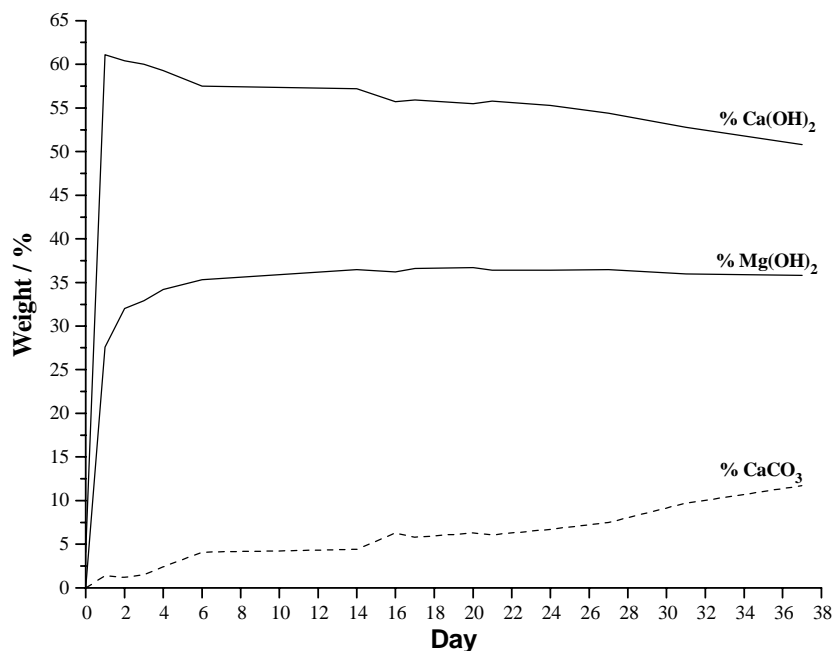
Fig. 7. Weight percentage of the compounds from TG results for DQ slaking (atmospheric environment).

Carbonation occurs via a solubility difference between the hydroxides and carbonates. Nevertheless, the occurrence of C and D in LCD becomes the carbonation favorable providing nucleating sites [17,18], and this fact prevails over the particle size, as is demonstrated by: the slow increment of calcite diffraction peaks in DQ through the test days as compared with the LCD, and D formation in DQ is virtually zero, whereas in LCD a slight D increase is observed due to the facilitated crystal growing.

3.2.2. Enclosed environment without CO_2

In this procedure, no differences have been observed by XRD in connection with the CH hydration rate: 24 h after the water addition all CaO is transformed into CH (Fig. 8).

Stirring clearly had an influence on the MgO hydration. Compared to LCD and DQ kept under atmospheric conditions and with discontinuous stirring, the MgO now reacts with water transforms into $Mg(OH)_2$ at a high rate: Fig. 8 shows the occurrence of significant amounts of $Mg(OH)_2$
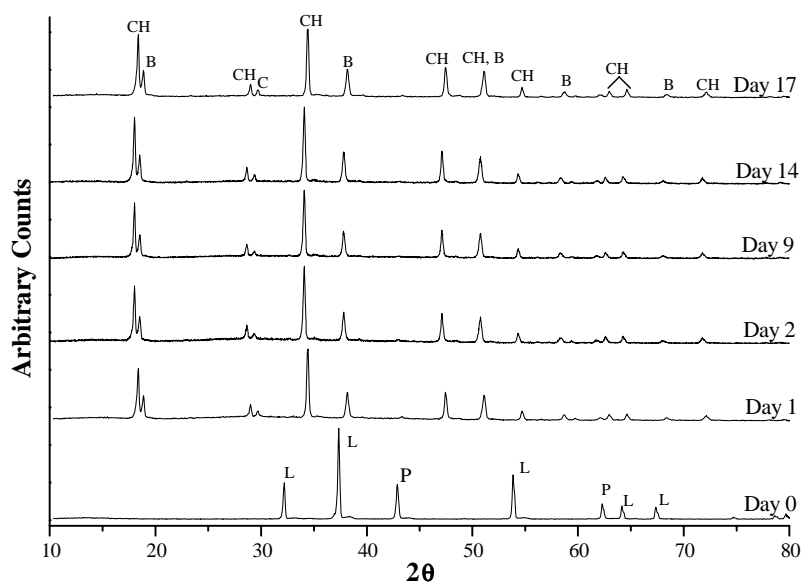

Fig. 8. XRD of DQ slaking evolution (enclosed environment without CO_2) at different days—B: brucite (ICDD 44-1482); C: calcite (ICDD 05-0586); CH: portlandite (ICDD 44-1481); P: periclase (ICDD 45-0946); L: calcium oxide (ICDD 37-1497).
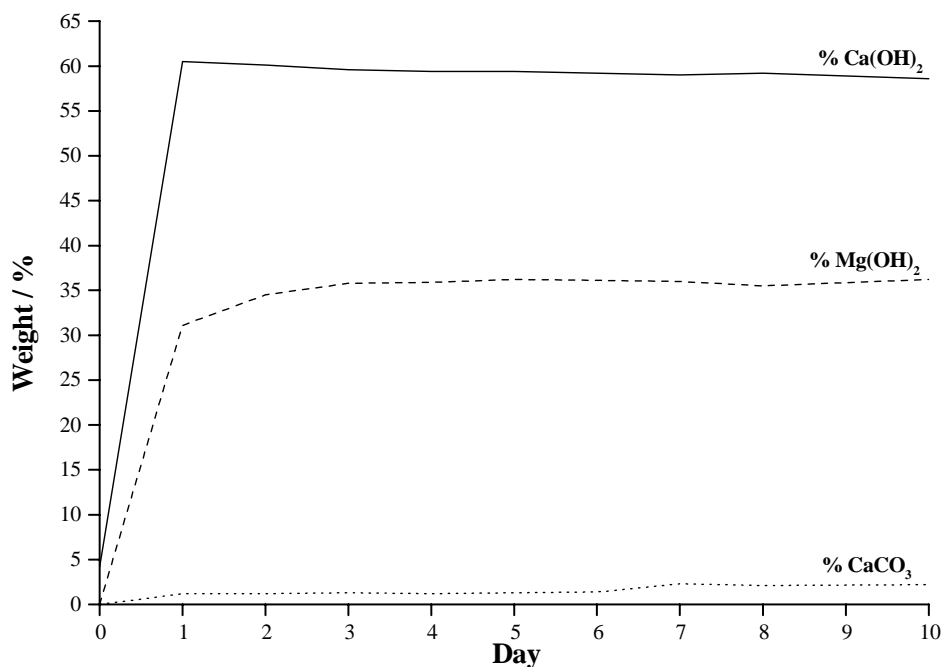
Fig. 9. Weight percentage of the compounds from TG results for DQ slaking (enclosed environment without CO_2) vs. time.

through its diffraction peaks 24 h after water addition. Practically all the MgO disappears after 24 h of reaction: only traces can be detected by XRD until day 2. This high rate of MgO hydration is attributed to the continuous stirring.

Calcite is detected by XRD (Fig. 8) and TG–DTA (Fig. 9) in small amounts since the first day of the reaction. This slight degree of carbonation can be due to the contact with: (i) atmospheric CO_2 of the lime powder before it was introduced into the glass reactor; (ii) a small amount of air in the reactor.

However, as expected, this C amount practically does not increase during the processing days due to the absence of CO_2.

Any magnesium carbonate has not been detected by XRD or TG–DTA analyses.

3.2.3. CO_2-rich environment

XRD analysis of the paste after 3 h of processing reveals the occurrence of CH and $Mg(OH)_2$, as products of CaO and MgO hydration, respectively. Nevertheless, some amount of MgO remains in the paste and a partial carbonation of CH is observed through the calcite formation. No evidence of the occurrence of any magnesium carbonate could be detected by TG–DTA analysis.

This is a non-equilibrium system because the CO_2 flow leads to a high CO_2 concentration, and the system evolves in a few hours giving, after one processing day, a paste with different composition (Fig. 10): a total CH carbonation was achieved as can be reflected by the C determination and the absence of CH. MgO also disappears, but $Mg(OH)_2$ is determined in traces. Therefore, total MgO hydration (as in the previous section) occurs when continuous stirring is applied. $Mg(OH)_2$ reacts and also transforms into nesquehonite ($MgCO_3\cdot 3H_2O$), a magnesium carbonate detected by XRD.

At two processing days, the paste reaches equilibrium, the amount of nesquehonite increases and brucite disappears.

The DTA curve in Fig. 11 shows a thermal behavior that could be related with the occurrence of a basic magnesium carbonate [7,13,19]. It shows, for an example, TG–DTA curves from the sample after 19 processing days. The endothermic doublet between 100 and 200 °C corresponds to the loss of two molecules of water of crystallization, apart from the excess moisture. Between 250 and 320 °C, the remaining molecule of water was eliminated, as can be seen from the endothermic peak (DTA curve) and the weight loss (TG curve) [8,13,20]. Thermal decomposition proceeds via decarbonation at ∼440 °C. A sharp exothermic phenomenon can be clearly distinguished at ∼500 °C (DTA curve). An identical exothermic peak has been observed for the thermal decomposition of hydromagnesite in previous work by our research group [5]. A pronounced weight loss is associated with the exothermic peak, as the DTG curve shows. At ∼550 °C, an endothermic decarbonation of $MgCO_3$ takes place, and finally at ∼900 °C calcite losses the CO_2 and transforms to CaO [20]. A further paper focuses on the thermal decomposition of nesquehonite.

The occurrence of nesquehonite as the result of $Mg(OH)_2$ carbonation deserves a careful discussion. No magnesite is obtained, as was stated in previous work [13,21], so the behavior of CH and $Mg(OH)_2$ during the carbonation is different.

In the present paper, nesquehonite was obtained during carbonation in CO_2 atmosphere of $Mg(OH)_2$. This results shows agreement with previous work, which also found
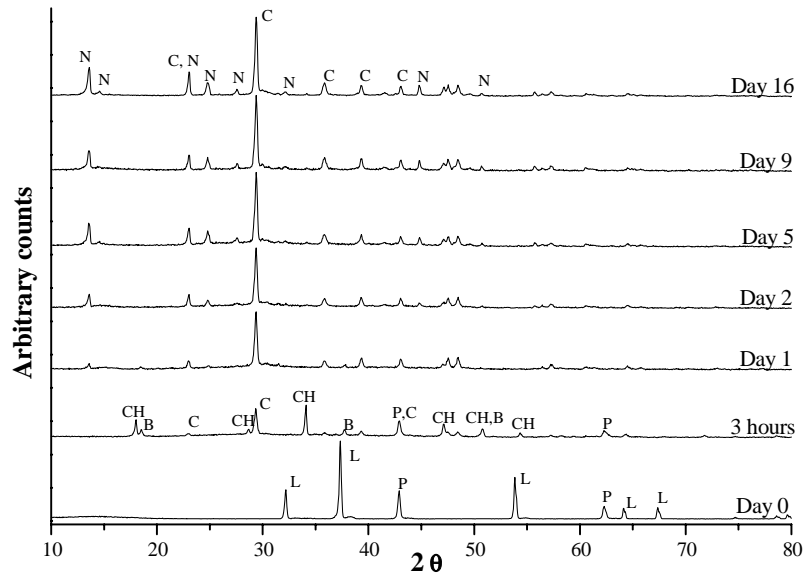
Fig. 10. XRD of DQ slaking evolution (CO_2-rich environment) at different days—B: brucite (ICDD 44-1482); C: calcite (ICDD 05-0586); CH: portlandite (ICDD 44-1481); P: periclase (ICDD 45-0946); L: calcium oxide (ICDD 37-1497); N: nesquehonite (ICDD 20-0669).

nesquehonite during carbonation at ambient temperature ($\sim$20 °C) [6,7,13,21]. Actually, nesquehonite is the stable hydrate below 52 °C and hydromagnesite is stable above this temperature.

It is necessary to explain why $Mg(OH)_2$ carbonates giving nesquehonite instead of magnesite. When the CO_2 pressure (P_{CO_2}) increases, the transformation of brucite into magnesite corresponds to the stable equilibrium state, as is shown in the thermodynamic model for the system $MgO–CO_2–H_2O$

[1]. However, the formation of magnesite (and also hydromagnesite and dolomite) may be kinetically inhibited, which explains the nesquehonite formation [1].

3.3. Evolution in atmospheric environment of the DQ powder

The analysis at different test days by XRD shows a gradual CaO slaking due to its reaction with atmospheric moisture
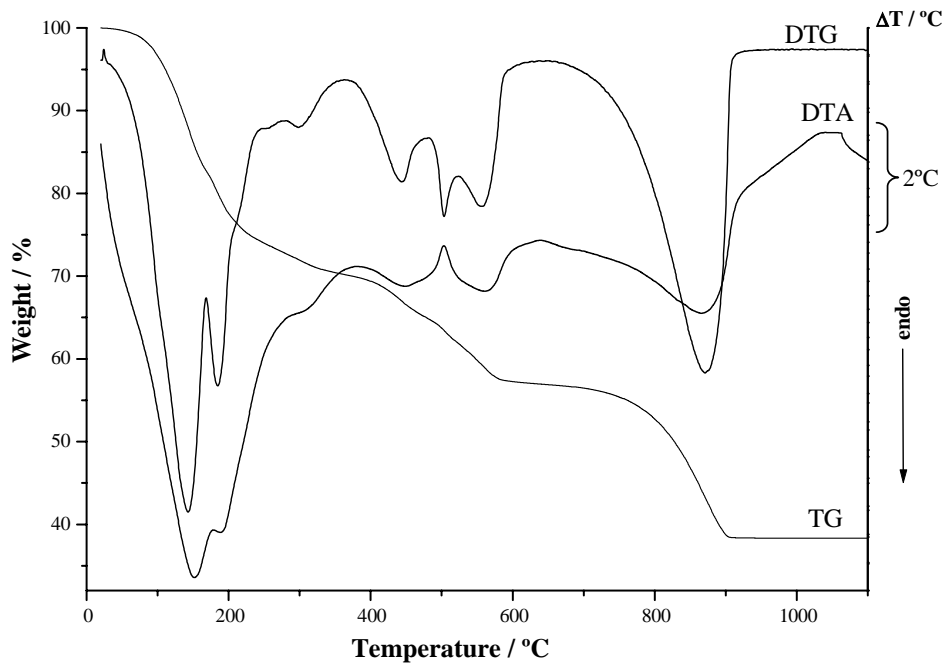

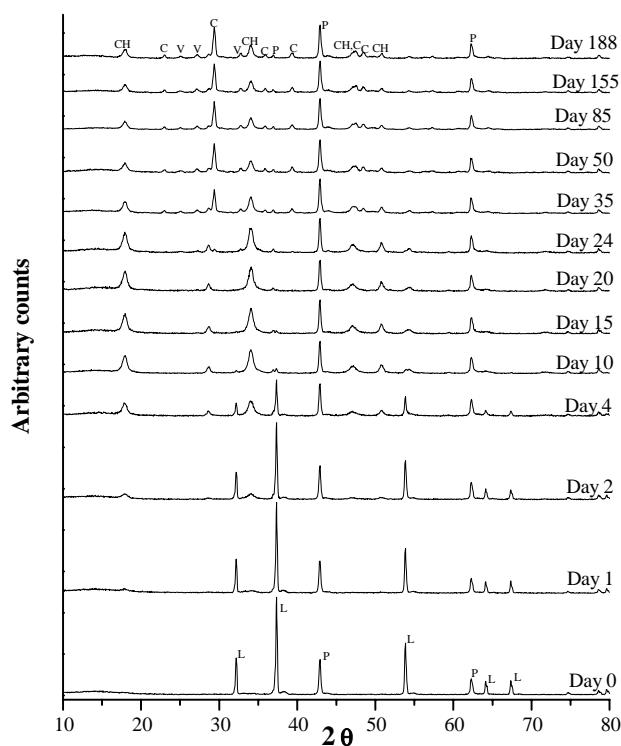Fig. 11. TG, DTG and DTA curves of DQ slaking (CO_2-rich environment) at 19 days.

Fig. 12. XRD of DQ powder (atmospheric environment) at different days—B: brucite (ICDD 44-1482); C: calcite (ICDD 05-0586); CH: portlandite (ICDD 44-1481); P: periclase (ICDD 45-0946); L: calcium oxide (ICDD 37-1497); V: vaterite (ICDD 01-1033).

Fig. 13. FT-IR spectrum of the DQ powder evolution (atmospheric environment) at 155 days—V: vaterite; C: calcite.

(Fig. 12). The amount of CH increases until a maximum after 10 days. Brucite was not found by XRD. However, from DTG curves, a slight weight loss at $\sim 380\,^\circ C$ can be observed, which can be attributed to the $Mg(OH)_2$ formation during 27 test days.

DQ powder carbonates forming different compounds that in pastes with excess of water. At 20 test days, traces of vaterite (thermodynamically unstable calcium carbonate) can be detected by XRD (Fig. 12). The amount of vaterite slightly increases up to 35 test days. Due to the small amount of vaterite formed, no significant changes in the CH amount are observed. Vaterite transforms directly and irreversibly into calcite, showing an exothermic peak at $\sim 460\,^\circ C$ [22,23]. Nevertheless, in the DTA curve this exothermic phenomenon cannot be checked due to the CH occurrence (with an exothermic dehydration at $\sim 480\,^\circ C$, which hides the vaterite transformation). FT-IR analysis confirms the vaterite occurrence through the presence of its most intense absorption bands at around ~ 745, ~ 850 and $\sim 875\,cm^{-1}$ (Fig. 13) [23,24].

Calcite is detected by XRD after 24 test days. The amount of calcite increases quickly in the next days. As a consequence the amount of CH decreases.

TG analysis allows one to detect smaller $CaCO_3$ amounts than with XRD, in fact non-crystalline forms can be detected by TG. These results show the $CaCO_3$ occurs since the first test day (Fig. 14). With XRD this $CaCO_3$ could not
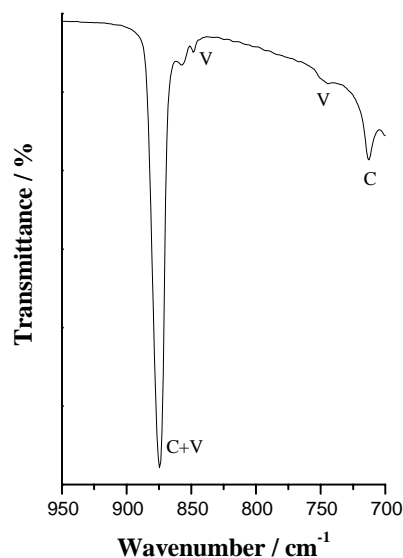
be identified due to the small amount and its low degree of crystallinity, as discussed below.

As mentioned already, the carbonation of CH requires to the CO_2 dissolution [17], so a certain degree of moisture is necessary in order to dissolve the atmospheric CO_2. This fact justifies the slow carbonation at the beginning of the DQ powder exposure.

At these early times, the first phase detected (by TG–DTA) is amorphous calcium carbonate. This is in agreement with previous reports that the Mg incorporation within amorphous calcium carbonate significantly retards transformation to crystalline phases [25].

Later the formation of the metastable polymorph (vaterite) is consistent with "the stage rule of Ostwald" [26]. The fact that vaterite forms demonstrates that the formation of vaterite is kinetically favorable under the present experimental conditions. Four test days later calcite appears, and it may be possible that the more soluble vaterite crystals dissolve while the less soluble calcite crystals nucleate and grow [27].

The amount of vaterite remains almost constant, whereas the amount of calcite quickly increases. This can be explained taking into account that:

(i) the syntaxial growth of calcite crystals, which improves the formation rate [17,18];
(ii) the rate of vaterite transformation controls the calcite crystallization, while the CH carbonation to give vaterite would proceed at a higher rate that keeps constant the amount of vaterite.

This is consistent with the initial occurrence of vaterite, and with the solution-mediated mechanism that takes place in order to transform vaterite into calcite. The dissolution of vaterite controls this transformation, because it is a very
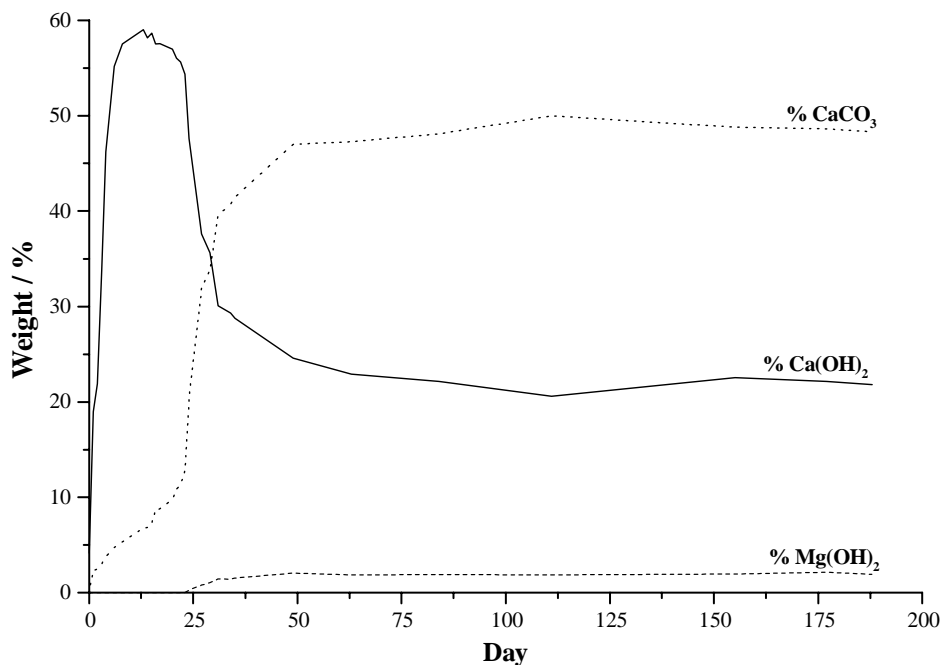
Fig. 14. Weight percentage of the compounds from TG results for DQ powder evolution (atmospheric environment) vs. time.

slow process compared with the crystallization of calcite. Therefore, the rate of transformation equals that of dissolution [26,27].

On the other hand, DTA curves show an exothermic effect at around 325 °C (Fig. 15) that can be associated with the reaction (Eq. (1)) [12]:

$$MgCO_3 + CaO \rightarrow MgO + CaCO_3 \qquad (1)$$
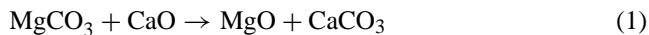
The reactivity of the calcium oxide determines the extent to which this reaction proceeds. Although magnesite is not checked in DQ powder, a certain degree of MgO carbonation could be expected or a solid–gas reaction (system $CaO–MgO–CO_2$) could take place, as suggested by Borchardt and Thompson [28].

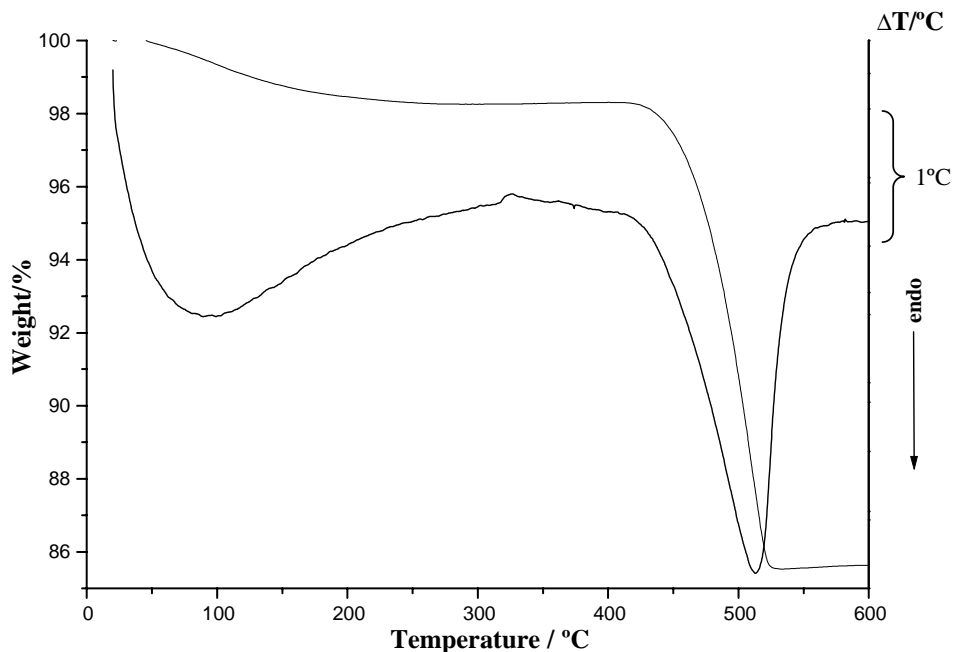Several facts support the occurrence of this exothermic peak:

Fig. 15. TG and DTA curves of DQ powder evolution (atmospheric environment) after nine processing days.
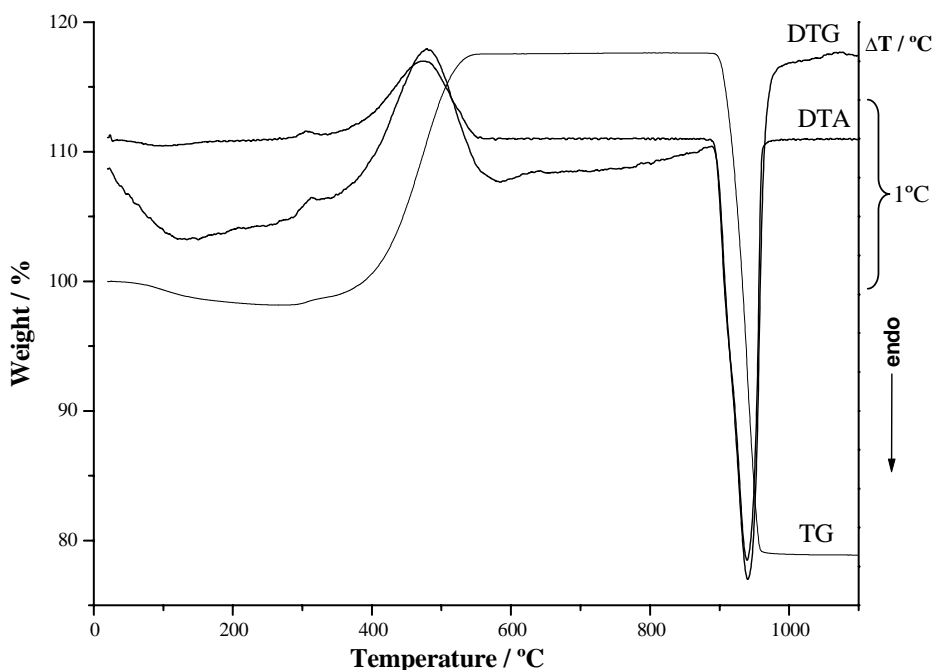
Fig. 16. TG, DTG and DTA curves of DQ powder evolution (atmospheric environment) after 12 processing days with a CO_2 flow of $100\,mL\,min^{-1}$.

(i) in the present work, the peak in DTA curve disappears when the amount of CaO decreases (between 20 and 24 test days);

(ii) the peak shows a great similarity with the results of a previous work [12] as a function of the calcination temperature of the lime;

(iii) Fig. 16 shows TG–DTA analysis performed in a CO_2 atmosphere ($100\,mL\,min^{-1}$) As expected, in a CO_2 atmosphere the peak turns out to be sharper. The endothermic peak related to the CH dehydration is masked by its exothermic carbonation [12]; the DTG curve reveals a slight weight increase (a rising peak) that could be caused by the included CO_2.

4. Conclusions

It has been proved that CaO hydrates at high rate in the presence of water. As expected, MgO shows a slower rate of hydration, which is strongly influenced by the particle size distribution and by stirring. Total MgO slaking was achieved with a continuous stirring. About the carbonation, CO_2 must be dissolved in water. This is a necessary and limiting process: CH carbonates in pastes with an excess of water, forming calcite. The rate of carbonation and the amount of this calcite have been improved by the syntaxial growing, as in LCD. In DQ powder, CH carbonates by another mechanism through vaterite formation. The difference probably lies in the high solubility of the metastable polymorph (vaterite) that hinders its formation in pastes with an excess of water. $Mg(OH)_2$ does not carbonate except:

(i) Slightly in a favorable syntaxial growing (in LCD forming a small amount of dolomite).

(ii) Strongly in a CO_2-rich environment: in this case, magnesite dolomite and hydromagnesite have not been detected, because these phases are kinetically inhibited. Nesquehonite ($MgCO_3 \cdot 3H_2O$) has been identified as the resulting magnesium carbonate.

Thermal studies (TG–DTA) have proved very useful in order to establish the hydration and carbonation reactions in dolomitic lime-based pastes.

References

[1] E. Königsberger, L.-C. Königsberger, H. Gamsjäger, Geochim. Cosmochim. Acta 63 (19/20) (1999) 3105–3119.

[2] S. Bruni, F. Cariati, P. Fermo, A. Pozzi, L. Toniolo, Thermochim. Acta 321 (1998) 161–165.

[3] S. Vecchio, A. Laginestra, A. Frezza, C. Ferragina, Thermochim. Acta 227 (1993) 215–223.

[4] R.G. Newton, J.H. Sharp, Stud. Conserv. 32 (1987) 163–175.

[5] C. Montoya, J. Lanas, M. Arandigoyen, I. Navarro, P.J. García Casado, J.I. Alvarez, Thermochim. Acta 398 (2003) 107–122.

[6] A. Botha, C.A. Strydom, Hydrometallurgy 62 (2001) 175–183.

[7] P.J. Davies, B. Bubela, Chem. Geol. 12 (1973) 289–300.

[8] A. Botha, C.A. Strydom, J. Therm. Anal. Calorim. 71 (2003) 987–995.

[9] Y. Sawada, K. Uematsu, N. Mizutani, M. Kato, Thermochim. Acta 27 (1978) 45–59.

[10] EN 459-1, Building lime, Part 1, Definition, Specification and Conformity Criteria, 2001.

[11] EN 196-2, Methods of testing cement, Part 2, Chemical Analysis of Cement, 1994.

[12] T.L. Webb, Oxides and hydroxides of monovalent and divalent, in: R.C. Mackenzie (Ed.), Differential Thermal Analysis, Academic Press, New London, 1970.

[13] T.L. Webb, J.E., Krüger, Carbonates, in: R.C. McKenzie (Ed.), Differential Thermal Analysis, Academic Press, London, 1970, pp. 238–266.

[14] Guía práctica de la cal y el estuco, Ed. de los Oficios, Leon, 1998.

[15] P.G. Caceres, E.K. Attiogbe, Miner. Eng. 10 (1977) 1165–1176.

[16] A.I. Fernández, J.M. Chimenos, M. Segarra, M.A. Fernández, F. Espiell, Hydrometallurgy 53 (1999) 155–167.

[17] O. Cazalla, Morteros de cal. Aplicación en el patrimonio histórico, PhD Thesis, Universidad de Granada, Granada, 2002, Unpublished (in Spanish).

[18] M. Heikal, M.H. El-Didamony, M.S. Morsy, Cem. Con. Res. 30 (2000) 1827–1834.

[19] N. Khan, D. Dollimore, K. Alexander, F.W. Wilburn, Thermochim. Acta 367–368 (2001) 321–333.

[20] Y. Sawada, K. Uematsu, N. Mizutani, M. Kato, Thermochim. Acta 32 (1979) 277–291.

[21] R.-M. Dheilly, Y. Sebaibi, J. Tudo, M. Queneudec, Can. J. Chem. 76 (1998) 1188–1196.

[22] M. Maciejewski, H.-R. Oswald, A. Reller, Thermochim. Acta 234 (1994) 315–328.

[23] J. Perić, M. Vučak, R. Krstulović, Lj. Brečević, D. Kralj, Thermochim. Acta 277 (1996) 175–186.

[24] N.V. Vagenas, A. Gatsouli, C.G. Kontoyannis, Talanta 59 (2003) 831–836.

[25] E. Loste, R.M. Wilson, R. Seshadri, F.C. Meldrum, J. Cryst. Growth 254 (2003) 206–218.

[26] M. Kitamura, J. Colloid Interf. Sci. 236 (2001) 318–327.

[27] N. Spanos, P.G. Koutsoukos, J. Cryst. Growth 191 (1998) 783–790.

[28] H.J. Borchardt, B.A. Thompson, J. Am. Chem. Soc. 82 (1960) 355–357.